

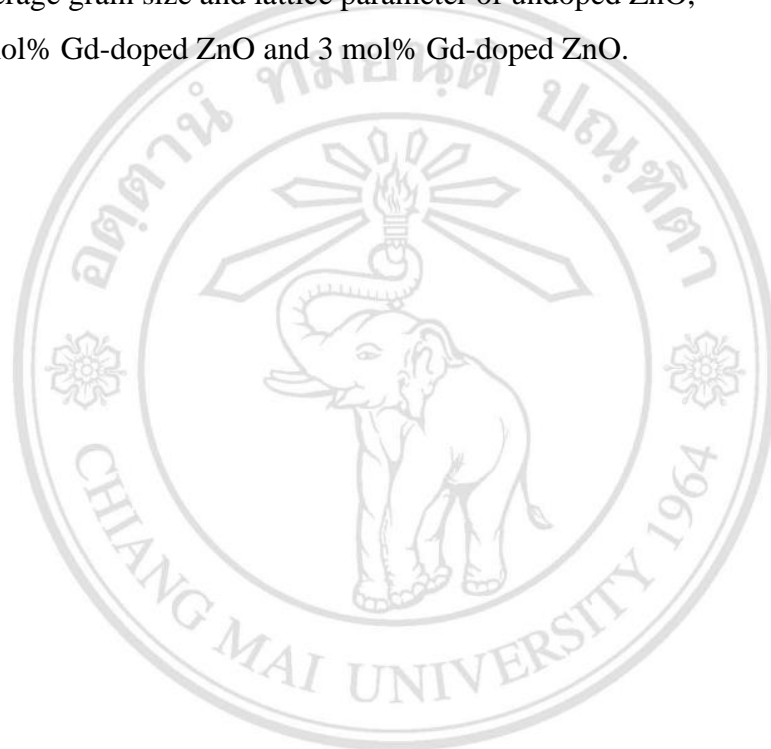
CONTENTS

	Page
Acknowledgement	c
Abstract in Thai	d
Abstract in English	e
List of Tables	h
List of Figures	i
List of Abbreviations	l
Statement of Originality in Thai	m
Statement of Originality in English	n
Chapter 1 Introduction	1
1.1 Introduction	1
1.2 Properties of zinc oxide and its applications	3
1.3 Photocatalytic activities and mechanism	11
1.4 Degradation mechanism of methylene blue	13
1.5 Sonochemical method	15
1.6 Literature Review	17
1.7 Research Objectives	21
Chapter 2 Experimental procedure	22
2.1 Chemical reagents and equipments	22
2.2 Synthesis methods	23
2.3 Photocatalytic testing	26
2.4 Characterization	28

Chapter 3 Results and discussion	33
3.1 Sonochemical synthesis, photocatalysis and photonic properties of Ce-doped ZnO nanostructures	33
3.2 Ultrasonic-assisted synthesis of Nd-doped ZnO for photocatalysis	44
3.3 Sonochemical synthesis of Dy-doped ZnO nanostructures and their photocatalytic properties	52
3.4 Synthesis and characterization of highly efficient Gd-doped ZnO photocatalyst irradiated with ultraviolet and visible radiations	66
Chapter 4 Conclusions	79
4.1 Sonochemical synthesis, photocatalysis and photonic properties of Ce-doped ZnO nanostructures	79
4.2 Ultrasonic-assisted synthesis of Nd-doped ZnO for photocatalysis	79
4.3 Sonochemical synthesis of Dy-doped ZnO nanostructures and their photocatalytic properties	80
4.4 Synthesis and characterization of highly efficient Gd-doped ZnO photocatalyst irradiated with ultraviolet and visible radiations	80
References	81
List of Publications	88
Appendix	89
Appendix A	89
Appendix B	92
Appendix C	97
Curriculum Vitae	123

LIST OF TABLES

	Page
Table 1.1 Chemical bonds energies in a methylene blue molecule.	13
Table 3.1 Average grain size and lattice parameter of undoped ZnO, 1 mol% Gd-doped ZnO and 3 mol% Gd-doped ZnO.	68



ลิขสิทธิ์มหาวิทยาลัยเชียงใหม่
Copyright© by Chiang Mai University
All rights reserved

LIST OF FIGURES

	Page
Figure 1.1 The cubic zinc-blende-type lattice (a), and hexagonal wurtzite-type lattice (b). In the wurtzite lattice, the atoms of the molecular base unit ($2\times\text{ZnO}$) are marked by red full circles and the primitive unit cell by green lines.	3
Figure 1.2 Mechanism of photocatalytic degradation of methylene blue.	12
Figure 1.3 Chemical structure of a methylene blue molecule.	13
Figure 1.4 The degradation path of the methylene blue molecule.	14
Figure 1.5 Frequency ranges of sound.	16
Figure 1.6 Generation of an acoustic bubble.	16
Figure 2.1 Schematic diagram used for preparing zinc oxide and lanthanide-doped zinc oxide by sonochemical method.	25
Figure 2.2 Schematic diagram used for photocatalytic testing.	27
Figure 2.3 X-ray diffractometer.	28
Figure 2.4 Fourier transform infrared spectrometer.	29
Figure 2.5 Raman spectrometer.	29
Figure 2.6 Field Emission Scanning Electron Microscope.	30
Figure 2.7 Transmission Electron Microscope.	31
Figure 2.8 Luminescence spectrometer.	31
Figure 2.9 UV-visible spectrometer.	32
Figure 3.1 XRD patterns of 0-3% Ce-doped ZnO synthesized by sonochemical method.	33
Figure 3.2 FTIR spectra of 0-3% Ce-doped ZnO synthesized by sonochemical method.	34
Figure 3.3 SEM image of (a) pure ZnO, (b) 1% Ce-doped ZnO, (c) 2% Ce-doped ZnO and (d) 3% Ce-doped ZnO, respectively.	35

Figure 3.4 (a) SEM image and EDX mapping of (b) Zn, (c) O and (d) Ce elements of as-synthesized 3% Ce-doped ZnO sample.	36
Figure 3.5 TEM images, HRTEM images and SAED patterns of (a, b) ZnO and (c, d) 3% Ce-doped ZnO.	37
Figure 3.6 (a) UV-visible absorption and (b) $(\alpha h\nu)^2$ vs $h\nu$ curve of samples.	38
Figure 3.7 (a) PL spectra of ZnO with and without Ce doping. Gaussian analysis of (b) ZnO and (c) 3% Ce-doped ZnO.	40
Figure 3.8 UV-visible absorption of MB test during UV light of using (a) ZnO and (b) 3% Ce-doped ZnO.	42
Figure 3.9 (a) Decolorization efficiency and (b) $\ln(C_0/C_t)$ for different lengths of UV irradiation time.	43
Figure 3.10 XRD patterns of Nd-doped ZnO nanoneedles.	44
Figure 3.11 FTIR spectra of 0-1% Nd-doped ZnO nanoneedles.	45
Figure 3.12 SEM images of (a–c) undoped, 0.5% Nd-doped and 1% Nd-doped ZnO, respectively.	46
Figure 3.13 TEM, HRTEM and SAED results of (a, b) pure ZnO and (c, d) 1% Nd-doped ZnO.	47
Figure 3.14 UV-visible absorption of MB dissolving in (a) ZnO and (b) 1% Nd-doped ZnO nanoneedles.	49
Figure 3.15 (a) Decolorization efficiency and (b) $\ln(C_0/C_t)$ for different lengths of UV irradiation time.	51
Figure 3.16 XRD patterns of 0–3% Dy-doped ZnO synthesized by sonochemical method over the 2θ range of (a) 20–60 deg and (b) 31–38 deg.	52
Figure 3.17 FTIR spectra of 0–3% Dy-doped ZnO synthesized by sonochemical method.	53
Figure 3.18 SEM images of (a) pure ZnO, (b) 1% Dy-doped ZnO, (c) 2% Dy-doped ZnO and (d) 3% Dy-doped ZnO.	54
Figure 3.19 (a) SEM image and (b–d) EDX mapping of Zn, O and Dy elements of the as-synthesized 3% Dy-doped ZnO, respectively.	55
Figure 3.20 TEM images, HRTEM images and SAED patterns of (a, b) ZnO and (c, d) 3% Dy-doped ZnO.	56

Figure 3.21	(a) UV-visible absorption and (b) the $(\alpha h\nu)^2$ vs $h\nu$ plots of pure ZnO and 3% Dy-doped ZnO.	58
Figure 3.22	(a) PL spectra of 0–3% Dy-doped ZnO and (b) Gaussian analysis of 3% Dy-doped ZnO.	59
Figure 3.23	UV-visible absorption of MB by UV light irradiation of the solutions containing (a) ZnO and (b) 3% Dy-doped ZnO as the photocatalytic materials.	63
Figure 3.24	(a) Decolorization efficiencies of MB and (b) pseudo-first-order kinetics of 0–3% Dy-doped ZnO during irradiation with UV light.	64
Figure 3.25	XRD patterns of undoped ZnO, and of 1 mol% Gd and 3 mol% Gd-doped ZnO synthesized by sonochemical method over the 2θ range of (a) 20–60 deg and (b) 30–38 deg.	66
Figure 3.26	Raman spectra of the undoped ZnO and 3 mol% Gd-doped ZnO synthesized by sonochemical method.	69
Figure 3.27	SEM images of (a) undoped ZnO, (b) 1 mol% Gd-doped ZnO, (c) 2 mol% Gd-doped ZnO and (d) 3 mol% Gd-doped ZnO.	70
Figure 3.28	TEM images and SAED patterns of (a, b) undoped ZnO, and (c, d) 3 mol% Gd-doped ZnO.	71
Figure 3.29	UV-visible absorption of MB by UV light irradiation of the solutions containing (a) undoped ZnO and (b) 3 mol% Gd-doped ZnO as the photocatalysts.	73
Figure 3.30	(a) Decolorization efficiencies of MB and (b) pseudo-first-order kinetics of the undoped ZnO, and of 1 mol% Gd, 2 mol% Gd and 3 mol% Gd-doped ZnO irradiated with UV light.	74
Figure 3.31	Decolorization efficiencies of MB in the different solutions: (a) pH = 5.54, 7 and 10 by 3 mol% Gd-doped ZnO and (b) pH = 10 by the recycled 3 mol% Gd-doped ZnO irradiated with UV light.	77
Figure 3.32	Decolorization efficiencies of MB in the different solutions: (a) pH = 5.54 and 10 by 3 mol% Gd-doped ZnO and (b) pH = 10 by the recycled 3 mol% Gd-doped ZnO irradiated with visible light.	78

LIST OF ABBREVIATIONS AND SYMBOLS

Å	Angstrom
°C	Degree Celsius
K	Kelvin
eV	Electron Volt
kHz	Kilohertz
MHz	Megahertz
M	Molarity
g	Gram
h	Hour
min	Minute
mg	Milligram
ml	Milliliter
nm	Nanometer
µm	Micrometer
MB	Methylene Blue
MW	Molecular Weight
UV	Ultraviolet
XRD	X-ray Diffraction
FTIR	Fourier Transform Infrared
PL	Photoluminescence
SEM	Scanning Electron Microscopy
FESEM	Field Emission Scanning Electron Microscopy
EDX	Energy Dispersive X-ray Spectroscopy
TEM	Transmission Electron Microscopy
HRTEM	High Resolution Transmission Electron Microscopy
SAED	Selected Area Electron Diffraction
JCPDS	Joint Committee on Powder Diffraction Standards

ข้อความแห่งการริเริ่ม

- 1) ในงานวิจัยนี้ได้สังเคราะห์โครงสร้างนาโนของซิงก์ออกไซด์และซิงก์ออกไซด์ที่เจือด้วยแลนทาไนด์โดยวิธีโซโนเคมีคอลได้สำเร็จ
- 2) สามารถใช้โครงสร้างนาโนของซิงก์ออกไซด์และซิงก์ออกไซด์ที่เจือด้วยแลนทาไนด์เป็นตัวเร่งปฏิกิริยาเชิงแสง โดยได้ศึกษาการเสื่อมสภาพของสารอินทรีย์ภายใต้รังสีอัลตราไวโอเล็ต
- 3) ได้เจือโครงสร้างนาโนของซิงก์ออกไซด์ด้วยแลนทาไนด์เพื่อเพิ่มประสิทธิภาพการเร่งปฏิกิริยาเชิงแสงของซิงก์ออกไซด์ได้สำเร็จ



ลิขสิทธิ์มหาวิทยาลัยเชียงใหม่
Copyright© by Chiang Mai University
All rights reserved

STATEMENTS OF ORIGINALITY

1. In this research, pure zinc oxide and lanthanide-doped zinc oxide nanostructures were successfully synthesized by a sonochemical method.
2. The as-synthesized zinc oxide and lanthanide-doped zinc oxide nanostructures were used as photocatalysts by measuring the degradation of organic compounds under ultraviolet (UV) radiation.
3. The photocatalytic performance of the photocatalysts was successfully improved by doping with lanthanide elements.



ลิขสิทธิ์มหาวิทยาลัยเชียงใหม่
Copyright© by Chiang Mai University
All rights reserved